Tribology International ■ (■■■■) ■■■–■■■

Contents lists available at ScienceDirect

Tribology International

journal homepage: www.elsevier.com/locate/triboint

Relation between roughness and processing conditions of AISI 316L stainless steel treated by ultrasonic shot peening

J. Marteau [a,*], M. Bigerelle [b], P.-E. Mazeran [a], S. Bouvier [a]

[a] Laboratoire Roberval, UMR 7334, Université de Technologie de Compiègne, Centre de Recherches de Royallieu, BP 20529, 60205 Compiègne Cedex, France
[b] Laboratoire Thermique, Energétique, Mise en forme, Production, UMR 8530, EA 4542, Université de Valenciennes et du Hainaut Cambrésis, Le Mont Houy, 59313 Valenciennes, France

ARTICLE INFO

Article history:
Received 23 July 2013
Received in revised form
12 June 2014
Accepted 16 July 2014

Keywords:
Multiscale roughness
Ultrasonic shot peening
stainless steel

ABSTRACT

This article assessed the roughness induced by ultrasonic shot peening. Surface properties of AISI 316L steel specimens were modified through the variation of ultrasonic shot-peening parameters (shot material, shot diameter, sonotrode amplitude vibration and coverage). Each surface was characterized using fifty surface roughness parameters and two types of robust Gaussian filter (low pass and high pass) associated with twenty one cut-off lengths. For each type of processing parameter, the most relevant roughness parameter and its corresponding length scale and filter were found. A linear relationship was identified between the four ultrasonic shot-peening parameters and the mean density of furrows with a coefficient of determination equal to 0.97.

1. Introduction

Shot peening is a mechanical surface treatment widely used in automotive and aerospace industries to enhance the fatigue life of mechanical parts [1,2]. In this process, many small and hard particles, called shots, are projected at high velocities onto the sample. The multiple impacts plastically deform the material surface and induce an in-plane compressive residual stress field near the surface.

Several other surface deformation processes have been recently developed such as Surface Mechanical Attrition Treatment (SMAT) [3], ultrasonic impact peening, laser peening [4], ball and burnishing [5] or ultrasonic shot peening technique [6]. The latter, unlike conventional shot-peening, consists in energizing the shots using a sonotrode vibrating at ultrasonic frequency, instead of using compressed air or centrifugal effects.

All these treatments aim at increasing the material fretting wear resistance [7,8]. However, the impacts usually induce increasing surface roughness that can accelerate crack nucleation and can thus decrease the fatigue life of the material [9].

As a consequence, many researchers have taken interest in the evolution of the material roughness after the surface mechanical treatment. Two main topics can be identified in the literature:

(i) Some researchers try to assess the influence of various surface treatments on material roughness. For instance, Maawad et al. [10] compared the effects of shot peening, ball burnishing, laser shock peening and ultrasonic shot peening on the surface roughness of an α-titanium alloy, using the average absolute value of the five highest peaks and the five lowest valleys over the cut-off length. Gao [11] explored the effects of shot peening and laser peening on the fatigue life by determining the stress concentration factor K_t, proposed by [12]. The latter is built using the maximum peak-to-valley height and the mean spacing of adjacent local peaks.
(ii) Other researchers observe the impact of the surface treatment conditions on the material roughness. Arifvianto et al. [13] investigated the effect of SMAT on the roughness of AISI 316L stainless steel, using various combinations of processing parameters (motor speed, treatment duration, ball diameter, ball number). Similarly, Mordyuk and Prokopenko [14] assessed the effect of the duration of ultrasonic impact peening on material roughness.

The one-dimensional average roughness R_a is the most widely used parameter to describe roughness, as shown in Table 1. However, the use of this sole parameter may not enable to thoroughly characterize all the features of the topography. Thus, some researchers chose to use additional roughness parameters. For instance, the

* Corresponding author. Tel.: +33 3 44 23 73 34; fax: +33 3 44 23 49 84.
E-mail address: julie.marteau@utc.fr (J. Marteau).

http://dx.doi.org/10.1016/j.triboint.2014.07.013
0301-679X/

Table 1
Examples of surface treatments and materials examined in the literature and the corresponding roughness parameters used to characterize the topography change.

Surface treatment	Material	Roughness parameters	Reference
Blasting	Low carbon steel	R_a	[27]
Blasting	AISI 316 LVM stainless steel	S_a, S_q, S_{sk}, S_{ku}, S_z, S_{bi}, S_{ci}, S_{vi}	[16]
SMAT	AISI 316L	R_a	[11]
SMAT	Alloy 718	R_a, R_{max}	[14]
SMAT	AISI 304 stainless steel	R_a, R_z	[13]
Shot peening	Low alloy steel	R_a, R_z, R_c, R_{sk}, R_{ku}	[15]
Shot peening, laser peening	7050-T7451 aluminum alloy	R_a, R_t, D_p	[9]
Shot peening, ultrasonic shot peening, laser shock peening and ball burnishing	Ti–2.5Cu alloy	R_z	[8]
Ultrasonic impact peening	Low carbon steel, AISI 321 stainless steel, titanium alloys	R_a	[12]
Surface nanocrystallization and hardening process	5052 Aluminum alloy	PV, R_q, R_a	[23]

Table 2
Processing conditions of the AISI 316L specimens.

Name	Shot material	Diameter (mm)	Sonotrode vibration amplitude (μm)	Coverage (%)
USP_1	304L	1	30	100
USP_2	304L	2	30	100
USP_3	304L	2	60	100
USP_4	100C6	2	60	100
USP_5	100C6	2	80	100
USP_6	100C6	2	60	1000
USP_7	100C6	2	60	10000
USP_8	100C6	1	60	100

maximum height R_z [8] or the maximum roughness depth R_{max} [15] were added to the observation of the R_a. To better characterize the height distribution of the peaks and the symmetry of the profile of a shot peened low alloy steel, Bagherifard et al. [16] also studied the evolution of the kurtosis R_{ku} and skewness R_{sk}.

Roughness parameters are numerous but seem to remain untapped. Furthermore, few studies question the relevance of the roughness parameters used to describe the effects of the tested surface treatment. Indeed, the choice of the roughness parameter is analyzed more comprehensively only in few cases, such as the search for biocompatibility [17].

In this work, three-dimensional roughness measurements are scrupulously analyzed. The aim is to identify the most relevant roughness parameters for the description of the effects of the processing parameters on the measured roughness. The investigated processing parameters are the shot material, shot diameter, sonotrode amplitude vibration and coverage (*i.e.* the percentage of the surface impacted once of more). A relation linking the obtained roughness to the combination of parameters used for the ultrasonic shot peening treatment is then searched.

This article is divided into four sections. Section 2 presents the material and the methods used in this study. Section 3 is devoted to the analysis of the roughness of the ultrasonically shot peened specimens: it discusses the identified relevant parameters and suggests a relationship between the topography and the design parameters used for the surface treatment. Section 4 concludes this work and suggests future topics related to this study.

2. Material and methods

2.1. Material and processing parameters

The material used in this study is AISI 316L stainless steel. The samples are cut from a 16 mm rod into 10 mm thick discs. This material is composed of a single austenitic phase. The 316L specimens are mechanically polished using an automatic grinding machine to get a mirror-like surface.

Ultrasonic shot peening was carried out using various processing parameters that are: the shot diameter (1 or 2 mm), the shot material (304L or 100C6), the coverage (100%, 1000% or 10,000%) and the amplitude vibration of the sonotrode (30, 60 or 80 μm). Coverage refers to the ratio of the surface area that is already impacted to the total surface area. Microscopic observations are used to assess coverage smaller than 100. Coverage larger than 100% is calculated using the processing time needed to reach 100% coverage. As an example, coverage equal to 200% means that the processing time is equal to twice the one needed to reach 100% coverage.

Eight specimens were studied from the combination of the shot diameter, the shot material, the coverage and the amplitude vibration of the sonotrode. The chosen processing parameters are presented in Table 2.

2.2. Roughness measurements

Surface roughness data were obtained using a three-dimensional non-contact optical profilometer (Zygo NewView™ 7300, Zygo Corp., USA). The white-light interferometer was used with a 20× objective. Its lateral resolution is equal to 71 nm while its vertical resolution is about 3 nm. Surfaces of 348 μm × 262 μm were measured. Using the stitching function, they were overlapped with a percentage of 20% to obtain surfaces of 1.19 mm × 0.891 mm (described by 2176 × 1632 points). Stitching enables to study large areas without decreasing the field of view. In this study, twenty stitched surfaces were randomly acquired for each specimen in order to ensure a good representativeness of the specimen roughness. Each 3D surface was flattened out using a polynomial of degree 3.

2.3. Multiscale roughness characterization

The surface topography resulting from the ultrasonic shot peening treatment was characterized through the coupling of a roughness parameter with a cut-off length and a filter. Fifty roughness parameters were calculated for each specimen in order to find the most relevant one. Some of the most significant roughness parameters calculated in this investigation are listed in Table 3. The roughness parameters are amplitude ones [18] such as the arithmetic mean deviation S_a, the root-mean-square deviation of the surface S_q. There are also hybrid parameters [18] like the density of summits S_{ds}, spatial parameters [19] like the texture aspect ratio S_{tr} or functional parameters [19] like the extreme peak height S_{xp}.

Please cite this article as: Marteau J, et al. Relation between roughness and processing conditions of AISI 316L stainless steel treated by ultrasonic shot peening. Tribology International (2014), http://dx.doi.org/10.1016/j.triboint.2014.07.013

Table 3
Examples of roughness parameters used in this study.

Amplitude parameters	
S_a	Arithmetic mean deviation
S_q	Root-mean-square deviation
S_{sk}	Skewness of the height distribution
S_{ku}	Kurtosis of the height distribution
Feature parameters	
S_{5V}	Five point pit height
S_{5P}	Five point peak height
Hybrid parameters	
S_{ds}	Density of summits
S_{fd}	Fractal dimension of the surface
Spatial parameters	
S_{al}	Auto-correlation length
S_{tr}	Texture-aspect ratio
Functional parameters	
S_{xp}	Extreme peak height
S_{mr}	Areal material ratio
S_{mc}	Inverse areal material ratio
Functional volume parameters	
V_v	Void volume
V_m	Material volume

As the values of the roughness parameters are directly linked with the cut-off length [20,21], twenty-one cut-off lengths ranging from 5 μm to 1100 μm were tested with two types of robust Gaussian filters [22]: a low-pass filter and a high pass filter. The use of these filters associated with different cut-offs allows to access to the waviness and roughness of the surfaces. Figs. 1 and 2 illustrate the effects of the coupling of a filter with a cut-off length.

2.4. Assessment of the relevance of the roughness parameters

The assessment of the most relevant parameter enabling the characterization of the effects of the different processing parameters is based on the coupling of an analysis of variance (ANOVA) with a recent resampling technique called Bootstrap [23].

The main aim of bootstrapping is to provide a confidence interval that enables to integrate the variability of roughness data into ANOVA. The idea of bootstrapping consists in generating a large number N ($N=1000$ in this study) of simulated bootstrap sets of samples of size K ($K=20$), from an experimental data set of the same size K. Each simulated bootstrap sample is a set of size K and is the result of the sampling of the experimental data set. The bootstrap sample is formed from the experimental data set using randomly sampling with replacement [24]. Thus, the bootstrap sample is not identical to the original experimental set as it contains different scores than the experimental set (some values can appear twice or more whereas others may not appear). This bootstrap set of 1000 values is then used to build an empirical probability density function for each roughness parameter S_i associated with a filter and a cut-off length.

This empirical probability density function is then used in the analysis of variance. For each parameter Si, the F-statistic [25] is calculated considering two or three classes of processing parameters (*e.g.* for the material ball, the classes are 304L or 100C6 whereas for the coverage, the classes are 100%, 1000% and 10,000%). In addition to the average and median of the F-statistic, the percentile 5% and 95% are determined as they can be used to compute a 90% confidence level. The F-statistic average is then used to rank the different roughness parameter S_i associated with a filter and a cut-off regarding their ability to characterize the two or three classes.

3. Results and discussion

3.1. Effect of the shot material

The shot material effect on roughness was studied using the specimens called USP_3 and USP_4 as their processing conditions are the same, except for the shot material. Using both specimens, the most relevant roughness parameter enabling to detect the shot material effect on topography was searched using the ANOVA method. The association of a roughness parameter with a type of filter and its cut-off length gave 2100 combinations that were classified according to their F-statistic average value, as depicted by Fig. 3.

The first-ranked parameter is the density of summits S_{ds} computed using a 19 μm cut-off with a high-pass filter. Thus, it is the most relevant parameter for the description of the shot material effect. The S_{ds} parameter belongs to the hybrid parameters describing the amplitude and spacing characteristics of the surface. It represents the number of peaks per unit area. According to [18], the peaks taken into account for the calculation of the S_{ds} parameter are detected by local neighborhood. A point is considered as a peak if it is higher than its eight neighbors.

Fig. 4 shows the distribution of this parameter for both types of shots, at the relevant scale. It is worth noting that the histograms are perfectly disconnected. It confirms the ability of this parameter to describe the shot effect on the specimen topography. If both distributions are assumed to be normal, then the average S_{ds} value for the specimen impacted with 100C6 shots is equal to 19,180 peaks/mm^2 with a standard deviation equal to 150 peaks/mm^2 while the S_{ds} value is equal to 11,360 peaks/mm^2 with a standard deviation equal to 45 peaks/mm^2 for the 304L shots. A lower density of peaks for the 304L shots means that the valleys are significantly larger than the ones obtained with the 100C6 shots.

With regard to the roughness parameters relevance, the arithmetic mean deviation S_a parameter first appears at the 51th position of the ranking composed of 2100 combinations. It also gave two well separated distributions as in Fig. 5 thus enabling to detect the effect of the change of shot material.

The hardness of the 304L shots and 100C6 shots is respectively equal to 3.6 GPa and 7.6 GPa, while the hardness of the 316L workpiece is approximately equal to 3.5 GPa. As the hardness of the 304L shot is of the same order of magnitude as the workpiece hardness, the 304L shots probably tend to be more deformed than the 100C6 shots during the impacts. Thus, they induce larger valleys and a smaller density of peaks than the 100C6 shots, as confirmed by the shapes of the profiles presented in Fig. 6.

Harada et al. [26] reported similar observations about the effect of the shot material on the surface roughness. They observed that the amount of plastic deformation generated after shot peening carburizing steel was considerably higher when using cemented carbide microshots instead of cast steel microshots. The larger roughness was attributed to the difference of hardness: cast steel microshots have a smaller hardness than the workpiece while the cemented carbide shots are significantly harder than the workpiece.

The S_{ds} parameter is statistically better than the S_a parameter because it collects more information thus enabling to better explain the effects of the shot material on the topography. Indeed, the S_{ds} parameter is calculated after the segmentation of the initial image of the topography, using the watershed algorithm. The latter was specifically designed to identify the significant hills and dales and remove the non-significant peaks and pits, as shown in

Please cite this article as: Marteau J, et al. Relation between roughness and processing conditions of AISI 316L stainless steel treated by ultrasonic shot peening. Tribology International (2014), http://dx.doi.org/10.1016/j.triboint.2014.07.013

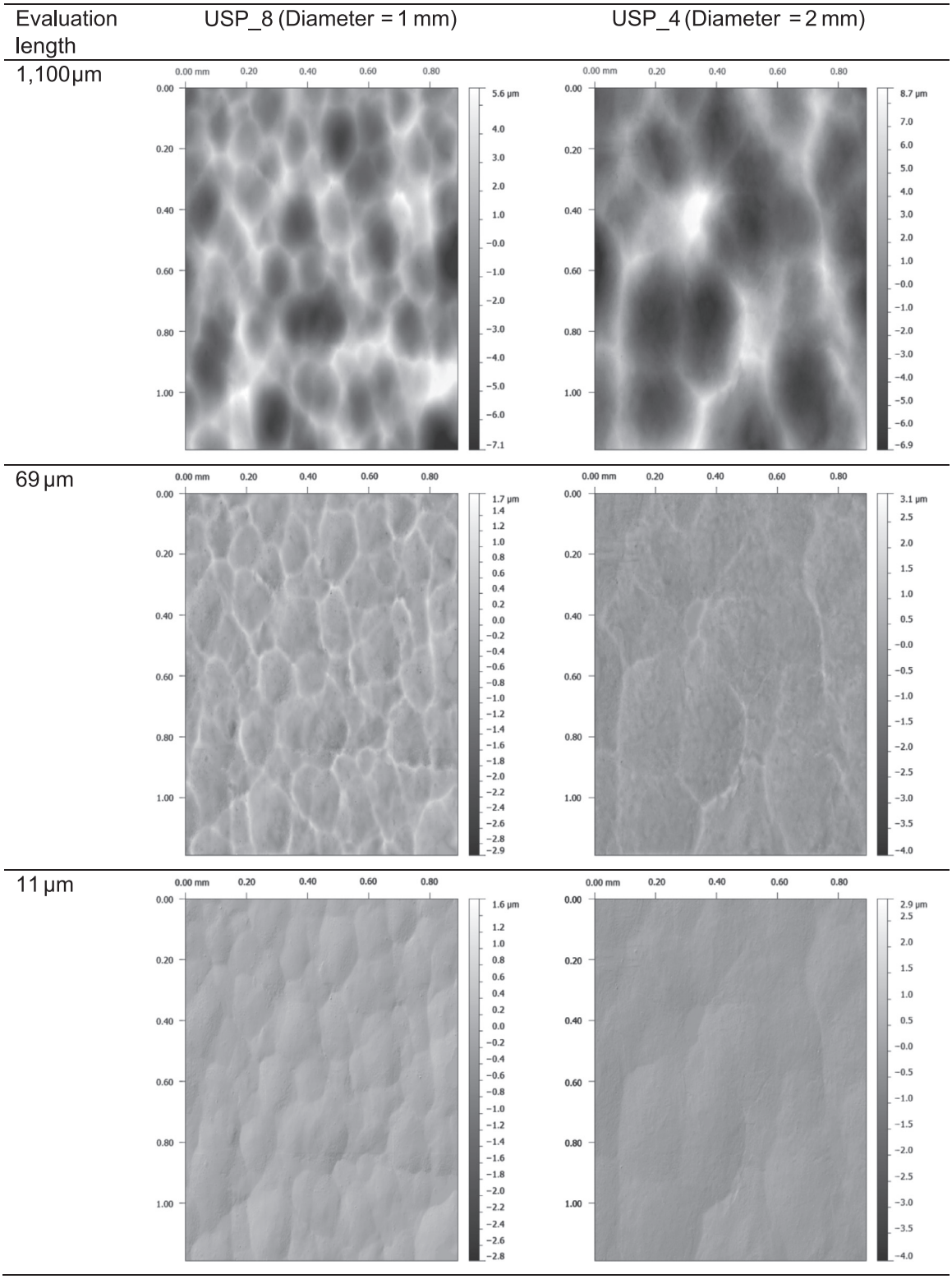

Fig. 1. Surface topographies of USP_4 (100C6 shots with a diameter of 2 mm) and USP_8 (100C6 shots with a diameter of 1 mm) with a high pass filter and cut-off lengths equal to 11 µm, 69 µm and 1100 µm.

Fig. 7. Indeed, as indicated by Li et al. [27] when analyzing sandblasted pure titanium, a surface showing relatively sparse summits has a lower S_{ds} value. More specifically, the density of summits is proportional to the number of residual impacts caused by the shots. This link between the S_{ds} parameter and the residual impacts of the shots fully justifies the first position of the S_{ds} parameter in the relevance. Furthermore, the impact diameters have a stochastic nature: they depend on the impact energy as well as the surface state (*i.e.* its ability to work-harden). The variation of the impact diameters leads to a variation of the topography that is detected in the ranking of the roughness parameters. Indeed, the first eighteen positions of the ranking are held by the density of summits associated with a large range of cut-off lengths. This large range of scales reflects the variation of

Please cite this article as: Marteau J, et al. Relation between roughness and processing conditions of AISI 316L stainless steel treated by ultrasonic shot peening. Tribology International (2014), http://dx.doi.org/10.1016/j.triboint.2014.07.013

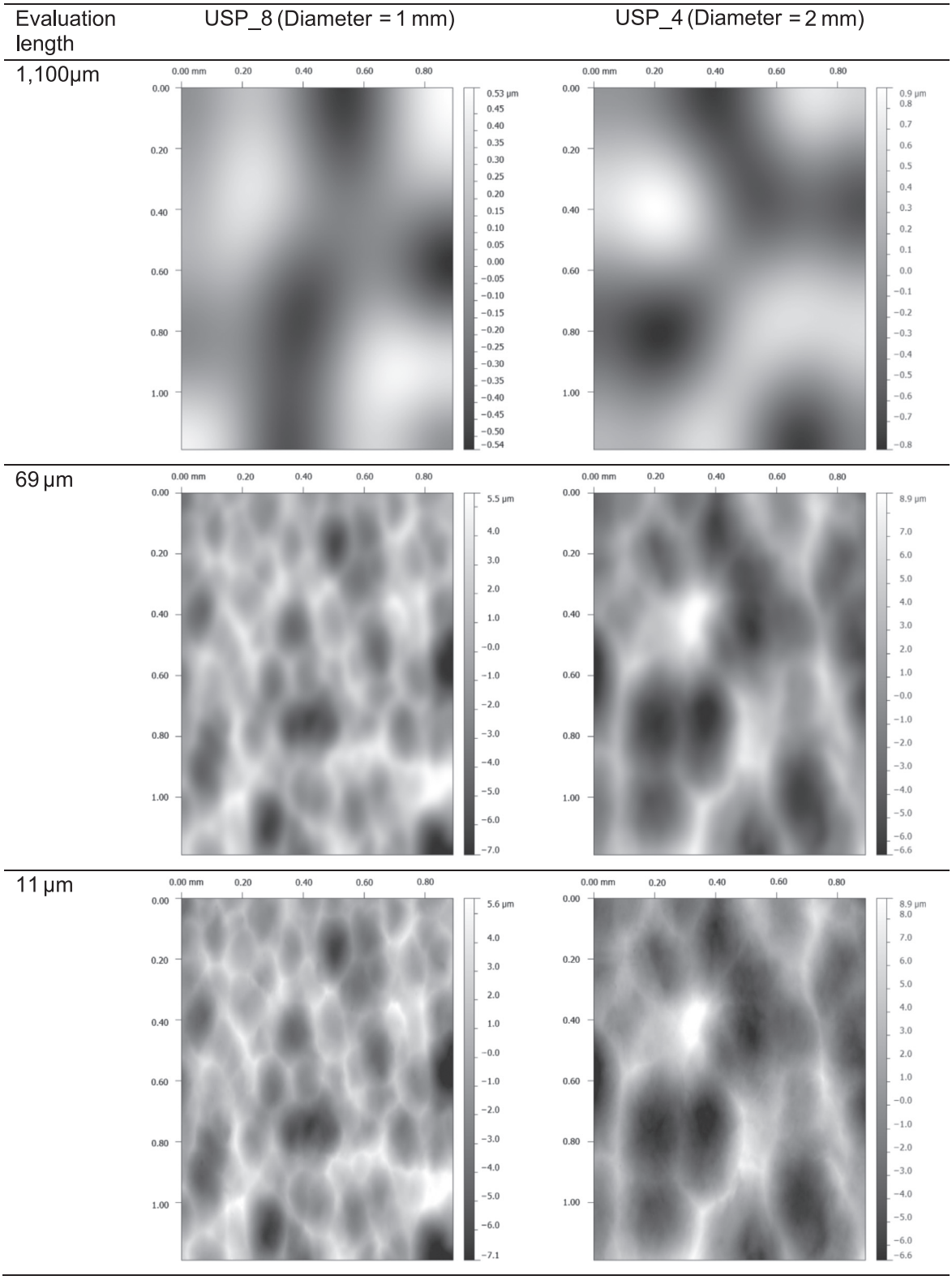

Fig. 2. Surface topographies of USP_4 (100C6 shots with a diameter of 2 mm) and USP_8 (100C6 shots with a diameter of 1 mm) with a low pass filter and cut-off lengths equal to 11 µm, 69 µm and 1100 µm.

impacts diameters, thus confirming the relevance of the density of summits for the description of the material effect on the topography.

It was shown that the most relevant roughness parameter for the description of the effect of shot material on the topography is the density of summits S_{ds}. This parameter was also shown to be more relevant than the arithmetic mean deviation of the surface S_a. It is worth noting that, as the surfaces of this study are isotropic, the arithmetic mean deviation of the surface (S_a) is equivalent to the arithmetic mean deviation of the profile (R_a). Surface parameters such as the density of summits (S_{ds}) have no equivalents in two-dimensional descriptions of the surface

Please cite this article as: Marteau J, et al. Relation between roughness and processing conditions of AISI 316L stainless steel treated by ultrasonic shot peening. Tribology International (2014), http://dx.doi.org/10.1016/j.triboint.2014.07.013

(*i.e.* using profiles). This fact emphasizes the specificities of surface roughness parameters compared to profile parameters.

3.2. Effect of the shot diameter

This section is dedicated to the analysis of the effect of the shot diameter on the topography of the specimens. It was investigated for two types of shot material: 100C6 and 304L steels. For the 304L steel, the diameter effect on the roughness was assessed through the analysis of the specimens USP_1 and USP_2 that were peened with shots having a diameter of 1 mm and 2 mm, respectively. The classification found through the use of the *F*-values showed that the mean density of furrows calculated with a cut-off length equal to 7 μm and a low pass filter is the most relevant roughness parameter for the characterization of the diameter effect. The mean density of furrows calculation is based on the segmentation of the topography measurements, using the watershed algorithm [28]. The latter leads to a partition of the examined image into dale motifs (as shown in Fig. 7) and locates their respective pits. This identification provides a linear topography whose length is measured and then divided by the considered area. The mean density of furrows is thus a measurement of furrows created by the shot impacts. An example of the determination of the mean density of furrows is given in Fig. 8.

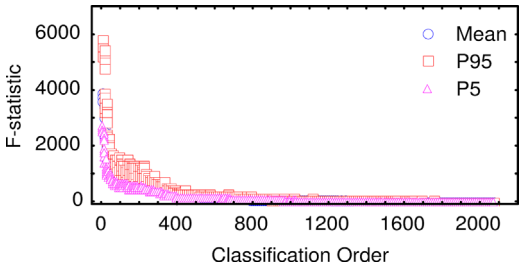

Fig. 3. Classification order of the relevance of the coupling of a roughness parameter with a cut-off length and a filter to describe the shot material effect on the surface topography.

The average value of the mean density of furrows is equal to 232 cm/cm^2 (with a standard deviation equal to 1 cm/cm^2) for the specimen peened with 2 mm diameter shots while it is about 347 cm/cm^2 (with a standard deviation of 1 cm/cm^2) for the one peened with 1 mm diameter shots. The arithmetic mean deviation S_a is only ranked 33. The S_a parameter is equal to 0.081 μm with a standard deviation equal to 0.001 μm for the 2 mm shots and is equal to 0.150 μm with a standard deviation equal to 0.001 μm for the 1 mm shots.

For the 100C6 shots, the roughness parameter that is ranked number 1 is also the mean density of furrows but with the use of a high pass filter and for a cut-off length equal to 122 μm. The mean density of furrows is approximately equal to 334 cm/cm^2 (with a standard deviation of 1 cm/cm^2) for the specimen peened

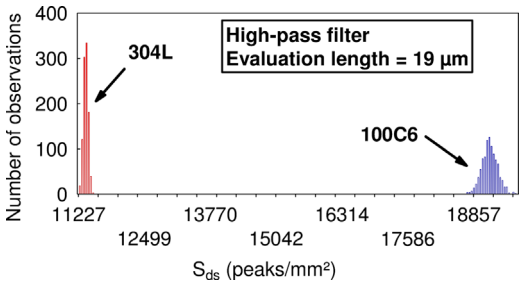

Fig. 4. Distribution of the density of summits S_{ds} values for the specimen treated with 100C6 shots (USP_4) and the one treated with 304L shots (USP_3) for a cut-off length of 19 μm, using a high-pass filter.

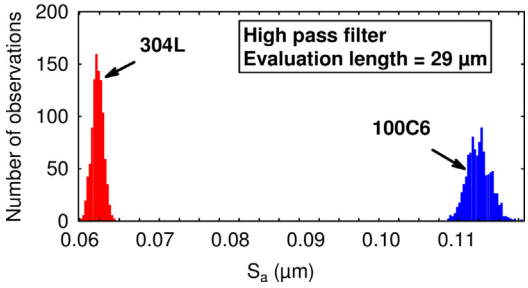

Fig. 6. Distribution of the arithmetic mean deviation S_a values for the specimen treated with 100C6 shots (USP_4) and the one treated with 304L shots (USP_3) for a cut-off length of 19 μm, using a high-pass filter.

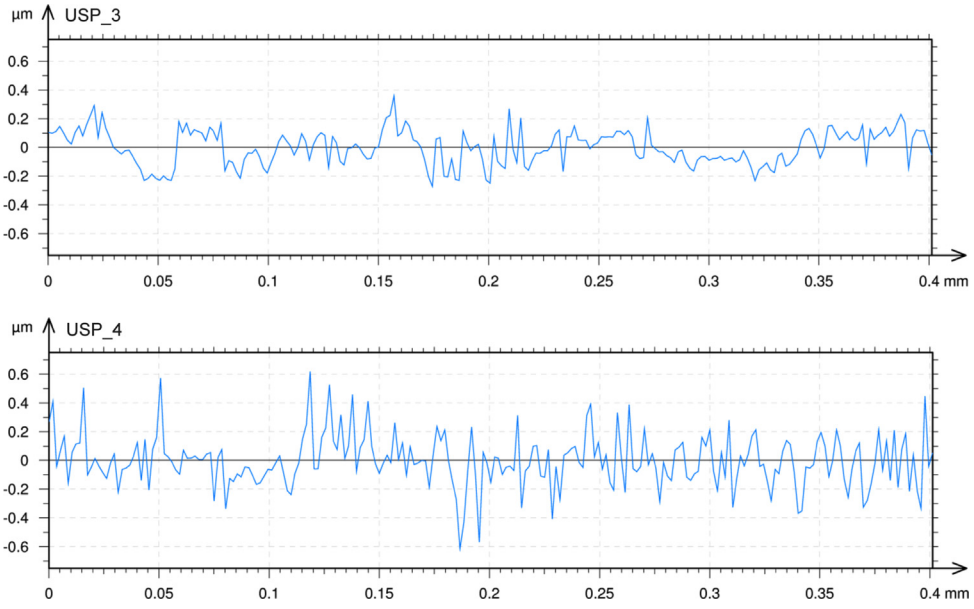

Fig. 5. Profiles of USP_3 and USP_4 with a cut-off length of 19 μm and a high pass filter.

Please cite this article as: Marteau J, et al. Relation between roughness and processing conditions of AISI 316L stainless steel treated by ultrasonic shot peening. Tribology International (2014), http://dx.doi.org/10.1016/j.triboint.2014.07.013

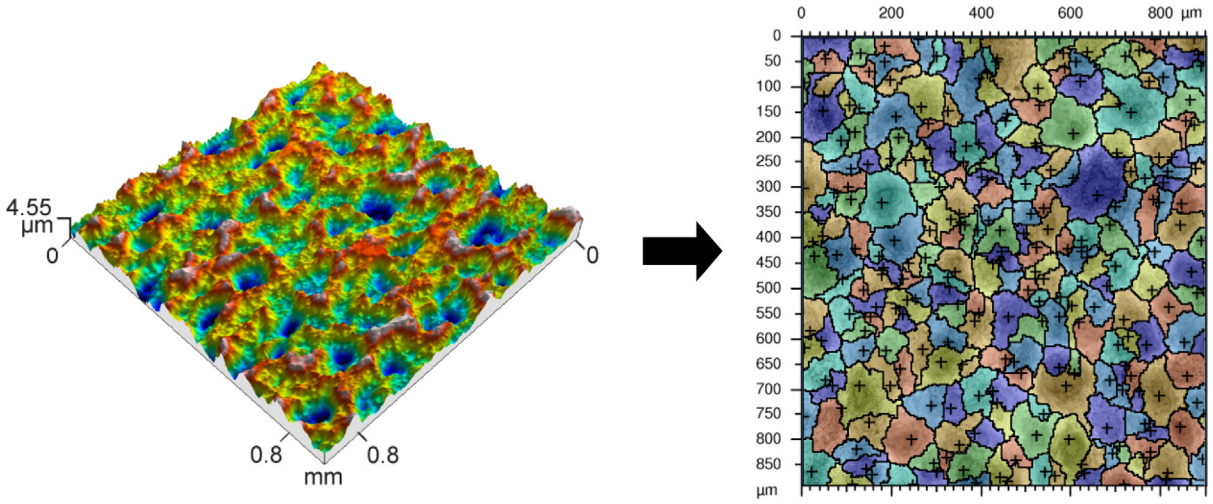

Fig. 7. 3D topography of the surface of the specimen called USP_1 and the corresponding determination of the motifs (the dales).

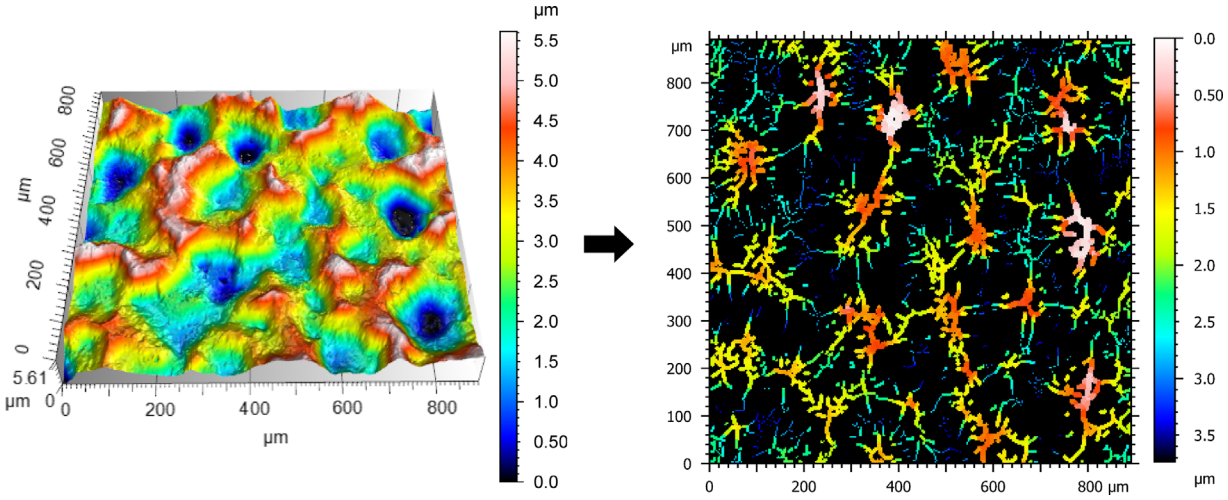

Fig. 8. 3D topography of the surface of the specimen called USP_2 and the corresponding determination of the furrows.

with shots having a 1 mm diameter (USP_8) while it is equal to 450 cm/cm^2 (with a standard deviation of 2 cm/cm^2) for the one peened with 2 mm diameter shots (USP_4). The arithmetic mean deviation S_a is ranked 96 in the classification of the relevance. The average S_a value is equal to 0.312 µm with a standard deviation of 0.002 µm for the 2 mm shots and is equal to 0.355 µm with a standard deviation of 0.002 µm for the 1 mm shots.

According to the previous results, an increase of the shot diameter tends to decrease the arithmetic mean deviation S_a, whatever the shot material. Conversely, the value of the mean density of furrows depends on the shot material as an increase of the shot diameter leads to an increase of the mean density of furrows for the 100C6 shots while it leads to a decrease of the mean density of furrows for the 304L shots.

The evolution of the S_a parameter can be easily understood: larger shot diameters induce larger dales and thus less peaks in average. Arifvianto et al. [13] found a similar trend when they treated AISI 316L steel using balls having a diameter of 3.18, 4.76 and 6.35 mm.

The mean density of furrows depicts the local variations of the topography. Figs. 9 and 10 present profiles of the specimens peened with 304L and 100C6 shots found using a cut-off length equal to 7 µm and a low-pass filter and a high-pass filter with a cut-off length of 122 µm, respectively. In Fig. 9, it can be seen that the specimen treated with 1 mm shots has more little peaks and pits than the one treated with 2 mm shots. In Fig. 10, this trend is reversed: the specimen treated with 100C6 shots having a diameter of 2 mm has more little variations than the one peened with 1 mm shots. As stated above, the hardness of the 304L shots is roughly similar to the one of the specimens. As the specimen and the 304L shots have similar hardness, the shots probably deform when they impact the treated material thus giving rise to smooth dales having few local peaks. On the contrary, the 100C6 shots are much harder than the specimens. Their shapes are thus less affected during the impacts, thus giving rise to higher deformations and to local variations in the specimen topography.

3.3. *Effect of the sonotrode vibration amplitude*

The search of an appropriate roughness parameter for the description of the effect of the sonotrode vibration amplitude on the specimen topography is successively made for the different shot material. First, the effect of the sonotrode vibration amplitude is investigated for the specimens shot with 304L steel balls. Two values of amplitudes were tested in this study: 30 µm (specimen USP_2) and 60 µm (specimen USP_3). The best parameter is the density of summits S_{ds} calculated with a low-pass filter and a cut-off length equal to 7 µm. The S_{ds} value is 530

Please cite this article as: Marteau J, et al. Relation between roughness and processing conditions of AISI 316L stainless steel treated by ultrasonic shot peening. Tribology International (2014), http://dx.doi.org/10.1016/j.triboint.2014.07.013

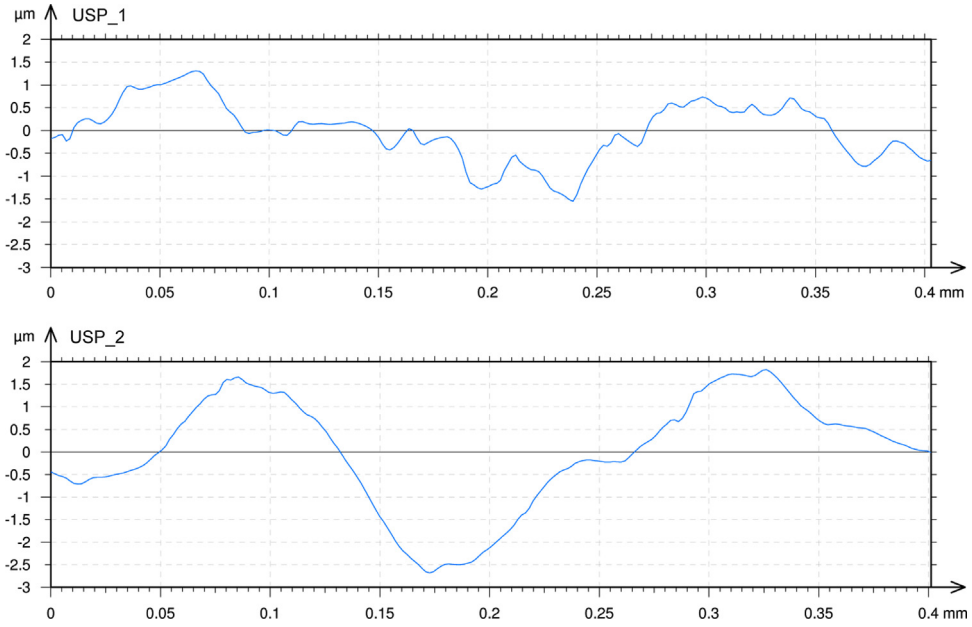

Fig. 9. Profiles of USP_1 and USP_2 with a cut-off length of 7 µm and a low pass filter.

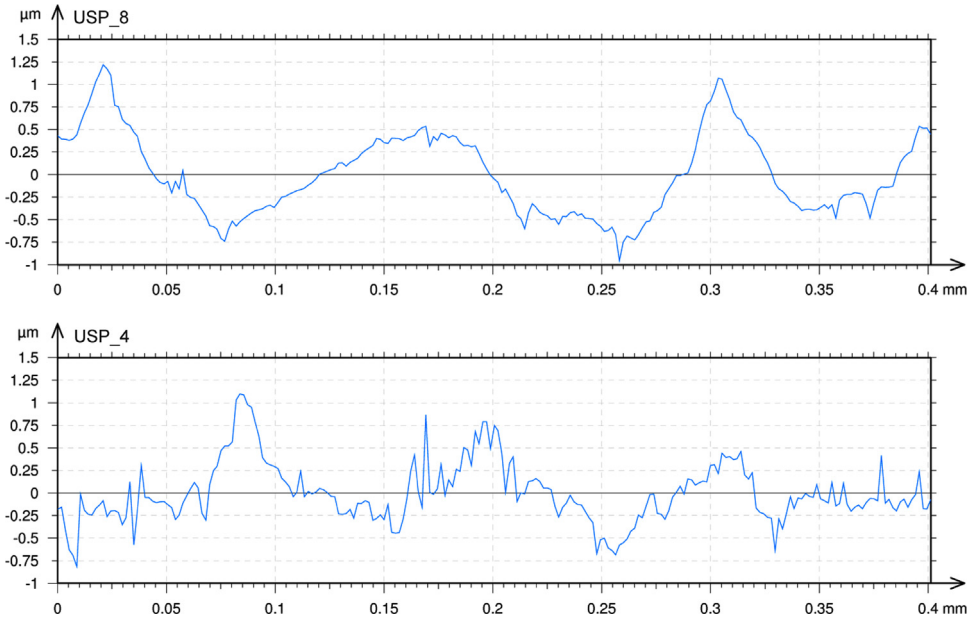

Fig. 10. Profiles of USP_8 and USP_4 with a cut-off length of 122 µm and a high pass filter.

peaks/mm² (with a standard deviation of 10 peaks/mm^2) for the 60 µm amplitude whereas it is equal to 920 peaks/mm^2 (with a standard deviation of 15 peaks/mm^2) for the 30 µm amplitude. The arithmetic mean deviation S_a parameter is ranked number 25. It gives a value of 1.01 µm (with a standard deviation of 0.02 µm) for the specimen treated with the 30 µm amplitude and 1.81 µm (with a standard deviation of 0.03 µm) for the one peened with the 60 µm amplitude. The use of higher vibration amplitude entails a decrease of the density of summits and an increase of the arithmetic mean deviation. Badreddine et al. [29] investigated the effects of the process parameters of ultrasonic shot peening on shot dynamics. They showed that the sonotrode amplitude is a key factor for the control of the normal speed of the impacts: higher impact velocity can be obtained using higher sonotrode amplitude. As a consequence, the increase of the vibration amplitude means that the impacts have higher kinetic energy, thus leading to higher deformations and higher dales or peaks in average. But, locally, the peaks and pits are much less numerous and large thus giving a lower density of summits, as illustrated by Fig. 11.

As for the 100C6 steel shots, the best parameter is found to be the extreme peak height S_{xp} with a high pass filter and a cut-off length equal to 7 µm. The extreme peak height is a functional parameter [19]. It is based on the areal material ratio, which is the bearing area ratio at a given height calculated from the mean plane. The S_{xp} parameter is the height at which an areal material ratio equal to 50% is satisfied, subtracted by the height at which an areal material ratio of 2.5% is achieved.

The S_{xp} parameter is equal to 0.277 µm (with a standard deviation of 0.002 µm) when the vibration amplitude is 60 µm while it is equal to 0.333 µm (with a standard deviation of 0.003 µm) for the 80 µm amplitude. As previously stated, the increase of the vibration amplitude induces the use of higher kinetic energy during the impacts thus leading to a global

Please cite this article as: Marteau J, et al. Relation between roughness and processing conditions of AISI 316L stainless steel treated by ultrasonic shot peening. Tribology International (2014), http://dx.doi.org/10.1016/j.triboint.2014.07.013

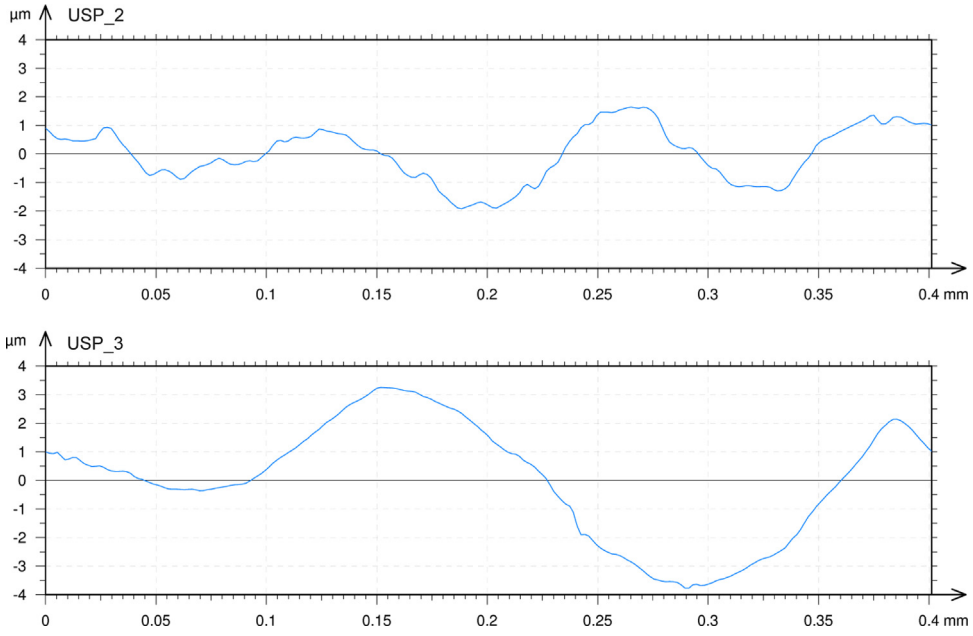

Fig. 11. Profiles of USP_2 and USP_3 with a cut-off of 7 µm and a low pass filter.

increase of the roughness. The S_{xp} parameter values follow this trend. This parameter is more relevant than commonly used parameters such as the arithmetic mean deviation because it implies the use of thresholds. Based on the Abbot curve, this parameter is computed by removing the largest peaks and valleys thus enabling to focus on the relevant peaks and valleys and eliminate outliers.

3.4. *Effect of coverage*

The effect of coverage is investigated using three specimens: USP_4, USP_6 and USP_7 having coverage equal to 100%, 1000% and 10,000%, respectively. The best roughness parameter depicting the coverage effect on topography is the mean density of furrows evaluated with a low pass filter and a cut-off length equal to 29 µm. As shown in Fig. 12, the mean density of furrows is equal to 175 cm/cm^2 for 100% coverage, 137 cm/cm^2 for 1000% coverage and 240 cm/cm^2 for 10,000% coverage. The standard deviation is equal to 1 cm/cm^2 whatever the examined coverage. There is a trend reversal: first the increase of coverage from 100% to 1000% leads to a decrease of the mean density of furrows, then from 1000% to 10,000% coverage, the mean density of furrows increases by a factor of 1.5.

Surface roughness evolution has been investigated as function of coverage or treatment duration by several researchers. However, different conclusions were drawn depending on the peening parameters. Dai et al. [30] identified three successive stages when severely plastically deforming aluminum alloy plates. In Stage I, the roughness characterized by the peak-to-valley parameter increases. This increase of roughness is due to newly created indents: the entire surface has not been entirely covered by the shot impacts. In Stage II, the peak-to-valley height decreases since the entire surface has been covered. This decrease is said to be caused by a continuous decrease of the peak regions while the depth of the valleys are not affected anymore by the impacts. Stage III is described as a steady state: there is a dynamic equilibrium between the generation of peaks and valleys and the reduction of the height of peaks. Mordyuk and Prokopenko [14] reported similar stages when observing the evolution of the Ra parameter as function of the ultrasonic impact peening duration.

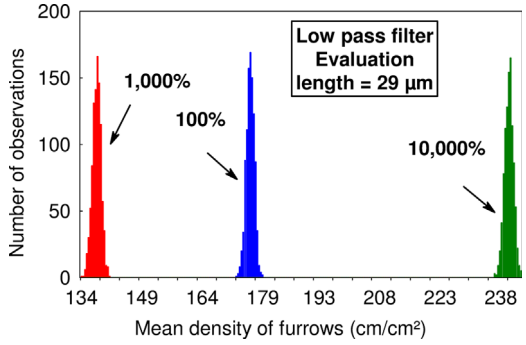

Fig. 12. Distribution of the mean density of furrows values for the specimen treated with 100% coverage (USP_4), 1000% coverage (USP_6) and the one treated with 10,000% coverage (USP_7) for a cut-off length of 29 µm, using a low-pass filter.

Miao et al. [31] conclusions were different from that of Dai et al. [30]. They identified only two stages when observing the variation of the peak-to-valley height with the increase of the number of shots. In Stage I, the peak-to-valley height increased almost linearly with the number of shots. During Stage II, the roughness increased at a much slower rate as many impacts were superimposed. Similar observations were made by Majzoobi et al. [32] and Bagherifard et al. [16]. Bagherifard et al. also emphasized the fact that depending on the chosen roughness parameter, the stabilization of the roughness could be observed earlier. Indeed, the average roughness parameter stabilized much earlier than the peak-to-valley parameter. This difference of number of stages may be explained by the achieved coverage (only 100% for Miao et al. [31] and 300% Bagherifard et al. [16]) or by the combination of processing parameters. Unfortunately, a lack of information on the parameters used by Dai et al. [30] prevent any calculation of the coverage using theoretical models such as the one developed by Kirk [33].

Given the literature results, the decrease of the mean density of furrows with the increase of the coverage from 100% to 1000% may correspond to the second stage described by Dai et al. [30]. As for the increase of roughness from 1000% to 10,000% coverage, it seems to be caused by a different phenomenon: a delamination of the strain-hardened layer of the specimen, as illustrated by Fig. 13.

Please cite this article as: Marteau J, et al. Relation between roughness and processing conditions of AISI 316L stainless steel treated by ultrasonic shot peening. Tribology International (2014), http://dx.doi.org/10.1016/j.triboint.2014.07.013

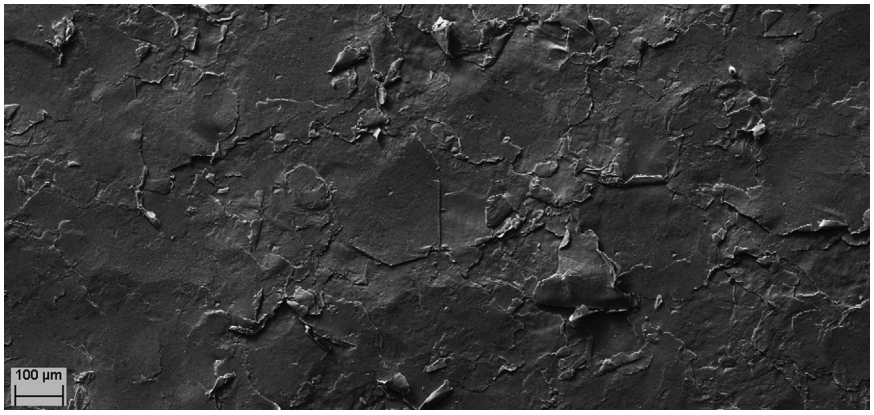

Fig. 13. Scanning electron microscopy image of the delamination of the strain-hardened layer (USP_7).

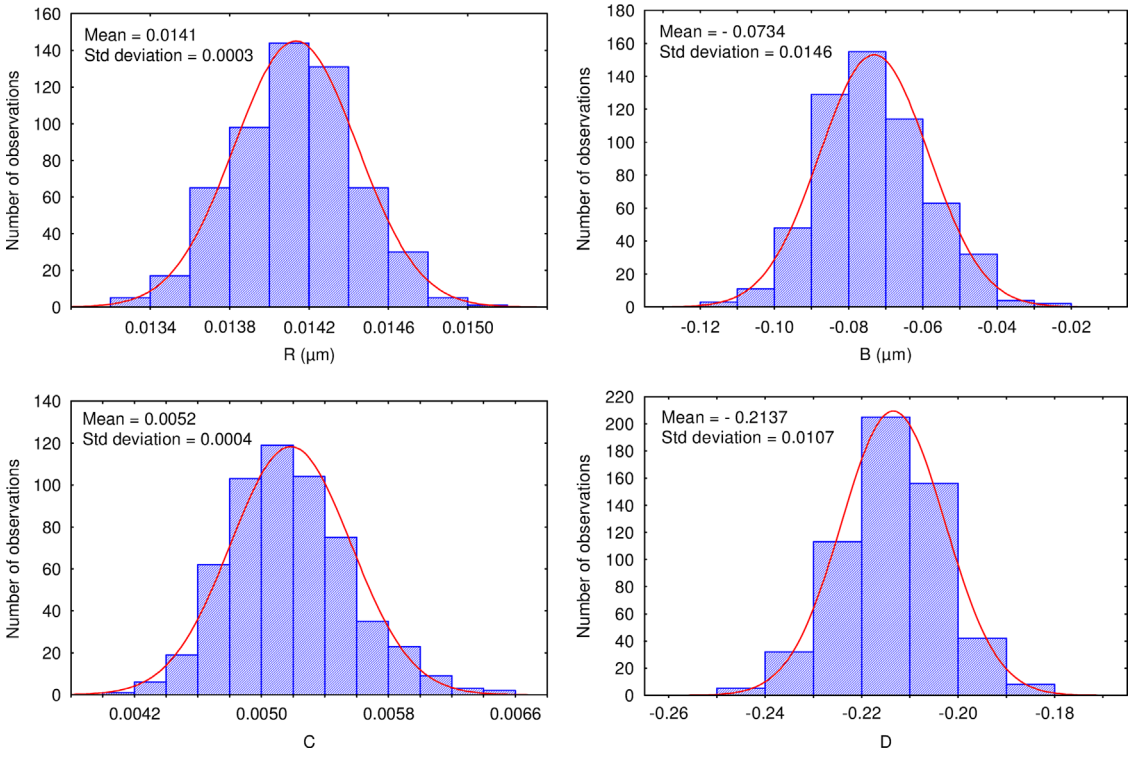

Fig. 14. Distribution of the model coefficient values.

The patterns observed in the previous figure are similar to the ones examined by Poorna Chander et al. [34] after over-blasting a steel substrate.

3.5. Creation of a predictive model

The method developed in this section consists in searching the best relation between the processing parameters (*i.e.* the shot diameter, the shot material, the sonotrode amplitude vibration and the coverage) and a roughness parameter associated with a filter and a cut-off length. To achieve this, the relation between the processing parameters and the obtained roughness is supposed linear as a first approximation. The relation giving the best coefficient of determination (0.97) is found using the Mean Depth of Furrows (MDF) with a high pass filter and a cut-off length of 122 µm:

$$\mathrm{MDF} = 0.75_{\pm 0.02} + 0.21_{\pm 0.01} d + 0.0052_{\pm 0.0004} c + 0.07_{\pm 0.01} b + 0.0141_{\pm 0.0003} r \quad (1)$$

where d, c, b and r are respectively: the ball diameter, the sonotrode vibration amplitude, the ball material and the coverage. For the shot material, 304L steel is represented by 1 while 100C6 steel is represented by 0.

Fig. 14 shows the distribution of the different coefficients of the previous equation. It can be seen that an addition of 1 to the coverage value increases the Mean Depth of Furrows of 0.014 µm. A 1 µm increase of vibration amplitude leads to a 0.0052 µm increase of the Mean Depth of Furrows. Conversely, a 1 mm increase of the ball diameter induces a 0.2 µm decrease and a gain of 1 for the ball material causes a drop of 0.08 µm.

The predicted Mean Depth of Furrows given by Eq. (1) is represented as a function of the measured Mean Depth of Furrows in Fig. 15. Despite some scattering of the points that stand for the bootstrap values of the Mean Depth of Furrows, a good prediction is achieved. Indeed, a linear relation having a coefficient of determination equal to 0.97 is found. It is worth noting that the coefficients of the predictive model are specific to the studied material *i.e.* to AISI 316L stainless steel. Indeed, the values of the

Please cite this article as: Marteau J, et al. Relation between roughness and processing conditions of AISI 316L stainless steel treated by ultrasonic shot peening. Tribology International (2014), http://dx.doi.org/10.1016/j.triboint.2014.07.013

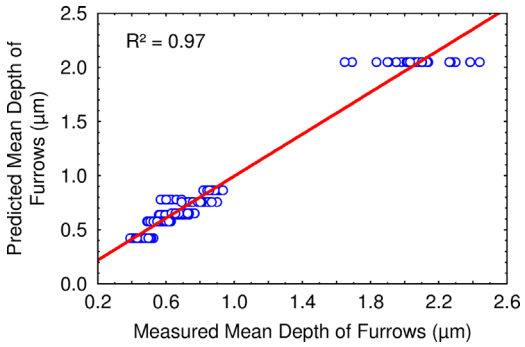

Fig. 15. Predicted mean depth of furrows as a function of the measured mean depth of furrows.

mean depth of furrows are dependent on the processing conditions as well as on the material behavior. As an example, Yin et al. [35] showed that the indented depth, which is proportional of the mean depth of furrows, depends on the strain state of materials. An increase of accumulated plastic strain of the material leads to a decrease of the indented depth.

The identified relation can help choosing the processing parameters when a certain roughness should be respected.

4. Conclusion

The multiscale analysis of roughness surfaces obtained by ultrasonic shot peening was performed by studying the values of fifty roughness parameters, 21 cut-off lengths and, high pass and low pass filters. The use of a statistical analysis enabled to identify a relevant parameter and its corresponding cut-off length and filter for each type of processing parameter. The effects of the variations of the shot diameter and coverage on the specimen topography were found to be best depicted by the mean density of furrows using a low pass filter and a cut-off length equal to 7 μm for 304L steel shots while a high pass filter and a cut-off length equal to 122 μm were found to be more relevant for 100C6 steel. As for the coverage, a cut-off length equal to 29 μm and a low pass filter were found to be more appropriate. The impact of the shot material was best described by the density of summits evaluated over 19 μm with a high pass filter. Finally, the effect of the vibration amplitude was found to be dependent on the shot material. Indeed, its effect was identified using the peak extreme height (with high pass filter and a cut-off length equal to 7 μm) for the 100C6 shots whereas the density of summits (with a low-pass filter and a cut-off length equal to 7 μm) was the relevant combination for the 304L balls.

Finally, the Mean Depth of Furrows, calculated using a cut-off length of 122 μm with a high pass filter, enabled to build a linear function with the different processing parameter *i.e.* the shot diameter, the shot material, the sonotrode vibration amplitude and the coverage. Such model could help choosing the correct processing parameters that increase fretting wear resistance while monitoring roughness at the same time.

References

[1] Liu KK, Hill MR. The effects of laser peening and shot peening on fretting fatigue in Ti–6Al–4V coupons. Tribol Int 2009;42:1250–62.
[2] Gao YK, Wu XR. Experimental investigation and fatigue life prediction for 7475-T7351 aluminum alloy with and without shot peening-induced residual stresses. Acta Mater 2011;59:3737–47.
[3] Roland T, Retraint D, Lu K, Lu J. Fatigue life improvement through surface nanostructuring of stainless steel by means of surface mechanical attrition treatment. Scr Mater 2006;54:1949–54.
[4] Masaki K, Ochi Y, Matsumura T, Sano Y. Effects of laser peening treatment on high cycle fatigue properties of degassing-processed cast aluminum alloy. Mater Sci Eng, A 2007;468–470:171–5.
[5] Hamadache H, Laouar L, Zeghib NE, Chaoui K. Characteristics of Rb40 steel superficial layer under ball and roller burnishing. J Mater Process Technol 2006;180:130–6.
[6] Liu G, Lu J, Lu K. Surface nanocrystallization of 316L stainless steel induced by ultrasonic shot peening. Mater Sci Eng, A 2000;286:91–5.
[7] Amanov A, Cho I-S, Kim D-E, Pyun Y-S. Fretting wear and friction reduction of CP titanium and Ti–6Al–4V alloy by ultrasonic nanocrystalline surface modification. Surf Coat Technol 2012;207:135–42.
[8] Sun Y. Sliding wear behaviour of surface mechanical attrition treated AISI 304 stainless steel. Tribol Int 2013;57:67–75.
[9] Curtis S, de los Rios ER, Rodopoulos CA, Levers A. Analysis of the effects of controlled shot peening on fatigue damage of high strength aluminium alloys. Int J Fatigue 2003;25:59–66.
[10] Maawad E, Brokmeier HG, Wagner L, Sano Y, Genzel C. Investigation on the surface and near-surface characteristics of Ti–2.5Cu after various mechanical surface treatments. Surf Coat Technol 2011;205:3644–50.
[11] Gao YK. Improvement of fatigue property in 7050–T7451 aluminum alloy by laser peening and shot peening. Mater Sci Eng, A 2011;528:3823–8.
[12] Li JK, Mei Y, Duo W, Renzhi W. An analysis of stress concentrations caused by shot peening and its application in predicting fatigue strength. Fatigue Fract Eng Mater Struct 1992;15:1271–9.
[13] Arifvianto B, Suyitno, Mahardika M, Dewo P, Iswanto PT, Salim UA. Effect of surface mechanical attrition treatment (SMAT) on microhardness, surface roughness and wettability of AISI 316L. Mater Chem Phys 2011;125:418–26.
[14] Mordyuk BN, Prokopenko GI. Ultrasonic impact peening for the surface properties' management. J Sound Vib 2007;308:855–66.
[15] Anand Kumar S, Ganesh Sundara Raman S, Sankara Narayanan TSN, Gnanamoorthy R. Influence of counterbody material on fretting wear behaviour of surface mechanical attrition treated Ti–6Al–4V. Tribol Int 2013;57:107–14.
[16] Bagherifard S, Ghelichi R, Guagliano M. Numerical and experimental analysis of surface roughness generated by shot peening. Appl Surf Sci 2012;258:6831–40.
[17] Pereda MD, Kang KW, Bonetto R, Llorente C, Bilmes P, Gervasi C. Impact of surface treatment on the corrosion resistance of ASTM F138-F139 stainless steel for biomedical applications. Proc Mater Sci 2012;1:446–53.
[18] Stout KJ, Matthia T, Sullivan PJ, Dong WP, Mainsah E, Luo N, et al. The developments of methods for the characterisation of roughness in three dimensions. Report EUR 15178 EN1993.
[19] Standardization IOf. ISO standard 25178. International Organization for Standardization; 2012.
[20] Bigerelle M, Giljean S, Mathia TG. Multiscale characteristic lengths of abraded surfaces: three stages of the grit-size effect. Tribol Int 2011;44:63–80.
[21] Marteau J, Mazeran PE, Bouvier S, Bigerelle M. Zero-point correction method for nanoindentation tests to accurately quantify hardness and indentation size effect. Strain 2012;48:491–7.
[22] Standardization IOf. ISO standard TS 16610-31. International Organization for Standardization; 2010.
[23] Efron B. Bootstrap methods: another look at the Jackknife. Ann Stat 1979; 7:1–26.
[24] Marteau J, Bigerelle M, Xia Y, Mazeran PE, Bouvier S. Quantification of first contact detection errors on hardness and indentation size effect measurements. Tribol Int 2013;59:154–62.
[25] Fisher RA. Statistical methods for research workers. London: Edinburgh Oliver and Boyd; 1928.
[26] Harada Y, Fukaura K, Haga S. Influence of microshot peening on surface layer characteristics of structural steel. J Mater Process Technol 2007;191:297–301.
[27] Li S, Ni J, Liu X, Lu H, Yin S, Rong M, et al. Surface characteristic of pure titanium sandblasted with irregular zirconia particles and acid-etched. Mater Trans 2012;53:913–9.
[28] Beucher S, Lantuejoul C. Use of watersheds in contour detection. In: International work-shop on image processing, real-time edge and motion detection/estimation. Rennes 1979.
[29] Badreddine J, Rouhaud E, Micoulaut M, Remy S. Simulation of shot dynamics for ultrasonic shot peening: effects of process parameters. Int J Mech Sci 2014;82:179–90.
[30] Dai K, Villegas J, Stone Z, Shaw L. Finite element modeling of the surface roughness of 5052 Al alloy subjected to a surface severe plastic deformation process. Acta Mater 2004;52:5771–82.
[31] Miao HY, Larose S, Perron C, Lévesque M. On the potential applications of a 3D random finite element model for the simulation of shot peening. Adv Eng Software 2009;40:1023–38.
[32] Majzoobi GH, Azadikhah K, Nemati J. The effects of deep rolling and shot peening on fretting fatigue resistance of aluminum-7075-T6. Mater Sci Eng, A 2009;516:235–47.
[33] Kirk D. Theoretical principles of shot peening coverage. Shot Peener 2005;19:28–30.
[34] Poorna Chander K, Vashista M, Sabiruddin K, Paul S, Bandyopadhyay PP. Effects of grit blasting on surface properties of steel substrates. Mater Des 2009;30:2895–902.
[35] Yin F, Hua L, Wang X, Rakita M, Han Q. Numerical modelling and experimental approach for surface morphology evaluation during ultrasonic shot peening. Comput Mater Sci 2014;92:28–35.

Please cite this article as: Marteau J, et al. Relation between roughness and processing conditions of AISI 316L stainless steel treated by ultrasonic shot peening. Tribology International (2014), http://dx.doi.org/10.1016/j.triboint.2014.07.013